

# A Combined Fit of X-ray/Neutron Total Scattering, EXAFS, and Electron Diffuse Scattering in *RMCPProfile*: User Manual

Victor Krayzman and Igor Levin

Materials Measurement Science Division,  
National Institute of Standards and Technology,  
Gaithersburg MD 20899

## 1. General Info

Local-structure scattering refinements using a simultaneous fit of x-ray/neutron total scattering, EXAFS, and diffuse scattering in electron diffraction are implemented as an extension to the *RMCPProfile* software **Version 6**. Users should refer to the main *RMCPProfile* manual for this version for details regarding RMC refinements using total scattering data alone. A user is expected to have a reasonable knowledge of EXAFS phenomena and be experienced in conventional EXAFS local-structure refinements. Relevant information, including tutorials, can be found at <http://cars9.uchicago.edu/~ravel/software/>. Likewise, a reasonable knowledge of electron diffraction is required.

The present software enables accurate EXAFS calculations for large atomic configurations with both single- and multiple-scattering of a photoelectron taken into account. The number of datasets is specified in the main input **\*.dat** file used by the *RMCPProfile* (asterisk refers to the stem filename). EXAFS data can be fitted either in  $k$ - or in  $r$ -space; the choice should be specified in the **\*.dat** file. EXAFS signal is calculated for an atomic configuration described in the **\*.rmc6f** file. All non-structural parameters that enter the EXAFS equation, such as scattering amplitudes and phase shifts, are calculated prior to refinements using the FEFF software (<http://leonardo.phys.washington.edu/feff/>). We strongly recommend self-consistent calculations of the cluster potential implemented in the FEFF8 (or free FEFF-light) version. The Artemis package (<http://cars9.uchicago.edu/~ravel/software/>) can be used to evaluate photoelectron scattering paths and to perform preliminary fitting of EXAFS data. A free version of FEFF included with Artemis does not support self-consistent calculations; therefore, a user needs to import the output files from FEFF8 (or FEFF-light) into Artemis manually.

Once the EXAFS option is selected in the **\*.dat** file, *RMCPProfile* will calculate an EXAFS signal for all types of absorbing atoms averaged over an atomic configuration. The calculations for each absorber are carried out as a sum over signals generated for single, double, and triple scattering of photoelectrons on the neighboring atoms (the types of scattering processes/paths to be included in a fit are selected by a user). The list of scatterers for each absorbing atom in the configuration is generated prior to a fit using the utility **SCAT\_ABS.exe**. After each atomic move, EXAFS is re-calculated for all the absorbers that include the moved atom as a scatterer. A list of absorbers around each atom is also generated prior to a fit using the utility **SCAT\_ABS.exe**. For fits with atom-swap moves,

the lists of absorbers and scatterers are updated after each swap move involving the absorbing and scatterer atoms, respectively. An effective scattering path length of about 5 Å ensures reasonable computation time.

The most advanced version of RMCProfile enables simultaneous fitting of X-ray & neutron total scattering, multiple EXAFS datasets, and single-crystal diffuse-scattering patterns (electrons or X-rays). The importance of including single-crystal diffuse scattering data in local-structure refinements is illustrated here using the synthetic data simulated for a cubic perovskite KNbO<sub>3</sub> with correlated atomic displacements (Appendix A4). The number of diffuse-scattering patterns that can be included in the fit is limited only by computing times.

## 2. EXAFS

### 2.1 Technical background

#### 2.1.1 Single Scattering

Single scattering (two-leg path) contributions to EXAFS for the  $i^{\text{th}}$  absorber and  $j^{\text{th}}$  scatterer are calculated according to a formula given in the FEFF manual:

$$\chi_{ij}^{(1)} = \frac{S_i^2 \Re(k) |F_j(\pi, k)|}{kr_{ij}^2} \sin(2kr_{ij} + 2\delta_i(k) - l\pi + \varphi_j(\pi, k)) \exp(-2r_{ij}/\lambda(k)) \quad (1)$$

where  $S_i^2$  is the amplitude reduction factor,  $\Re(k)$  is the total central-atom loss factor,  $r_{ij}$  is the interatomic distance,  $k$  is the photoelectron wave number,  $F_j(\pi, k) = |F_j(\pi, k)| \exp(\varphi_j(\pi, k))$  is the complex backscattering amplitude,  $[2\delta_i(k) - l\pi]$  is the total scattering phase shift for the absorbing atom, and  $\lambda(k)$  is the photoelectron mean free path.

Functions  $S_i^2$ ,  $\Re(k)$ ,  $2\delta_i(k) - l\pi$ ,  $\lambda(k)$ ,  $|F_j(\pi, k)|$  and  $\varphi_j(\pi, k)$  are calculated by FEFF. A utility program **EXAFS\_INTER.exe** is used to interpolate these functions on the  $k$ -mesh of the experimental data and store the parameters in the **\*.nsc1** file (see Section 5.1).

#### 2.1.2 Double and Triple Scattering

The exact equation for a double-scattering (i.e. a three-leg path, Fig. 1) contribution that involves an absorber  $i$  and scatterers  $j$  and  $n$  is expressed as:

$$\chi_{ijn}^{(2)} = \text{Im} \left\{ C(\mathcal{G}_{nij}) \frac{S_i^2 \Re F_j(\mathcal{G}_{ijn}, k) F_n(\mathcal{G}_{jni}, k)}{kr_{ij} r_{jn} r_{ni}} \exp[i(2kr_{\text{eff}} + 2\delta_i(k) - l\pi)] \exp\left[-\frac{2r_{\text{eff}}}{\lambda(k)}\right] \right\} \quad (2)$$

Here,  $r_{\text{eff}} = 1/2(r_{ij} + r_{jn} + r_{ni})$  is the effective scattering-path length,  $F_j(\mathcal{G}_{ijn}, k) = |F_j(\mathcal{G}_{ijn}, k)| \exp(i\varphi_j(\mathcal{G}_{ijn}, k))$  is the complex scattering amplitude for an atom  $j$

and the scattering angle  $\mathcal{G}_{ijn}$ , and  $C(\mathcal{G}_{nij})$  is the angle-dependent parameter (in the plane-wave approximation  $C(\mathcal{G}_{nij}) = \cos(\mathcal{G}_{nij})$ ).

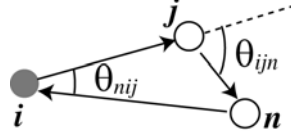


Fig. 1: A schematic representation of double scattering in a three-leg path. The scattering process involves an absorber  $i$  and scatterers  $j$  and  $n$ .

The FEFF code provides two real functions as an output:

$$F^{effective}(k) = \frac{|C(\mathcal{G}_{nij})F_j(\mathcal{G}_{ijn}, k)F_n(\mathcal{G}_{jni}, k)|}{r_{ij}r_{jn}r_{ni}} r_{eff}^2$$

$$\varphi^{effective}(k) = \arg C(\mathcal{G}_{nij})F_j(\mathcal{G}_{ijn}, k)F_n(\mathcal{G}_{jni}, k)$$

These functions can be substituted into Eq. (1) to calculate an EXAFS signal as implemented, for example, in the IFEFFIT/Artemis software. Similarly, in the present RMC calculations, the contribution of double scattering to EXAFS is calculated using the approximate formula:

$$\chi_{ijn}^{(2)} = \frac{S_i^2 \Re F_{jn}^{eff(2)}(\mathcal{G}, k)}{kr_{ij}r_{jn}r_{ni}} \sin(2kr_{eff} + 2\delta_i(k) - l\pi + \varphi_{jn}^{eff(2)}(\mathcal{G}, k)) \exp(-2r_{eff}/\lambda(k)), \quad (3)$$

where the effective amplitude factor is

$$F_{jn}^{eff(2)}(\mathcal{G}, k) = \frac{|C(\mathcal{G}_{nij})F_j(\mathcal{G}_{ijn}, k)F_n(\mathcal{G}_{jni}, k)|}{r_{0ij}^2} r_{0ij}r_{0jn}r_{0ni},$$

and the effective phase correction is

$$\varphi_{jn}^{eff(2)}(\mathcal{G}, k) = \arg(C(\mathcal{G}_{nij})F_j(\mathcal{G}_{ijn}, k)F_n(\mathcal{G}_{jni}, k)).$$

Here  $r_{0ij}$  is the distance between the atoms  $i$  and  $j$  in the cluster used in FEFF calculations.

Similarly, the contributions of the triple-scattering paths (Fig. 2) that involve either one or two scatterers are calculated according to the approximate formulae:

$$\chi_{ijn}^{(3)} = \frac{S_i^2 \Re F_{jn}^{eff(3)}(\mathcal{G}, k)}{kr_{ij}^2 r_{jn}^2} \sin(2kr_{eff} + 2\delta_i(k) - l\pi + \varphi_{jn}^{eff(3)}(\mathcal{G}, k)) \exp(-2r_{eff}/\lambda(k)) \quad (4a)$$

$$r_{eff} = r_{ij} + r_{jn} \text{ (Fig. 2a)}$$

$$\chi_{ij}^{(3)} = \frac{S_i^2 \Re F_j^{eff(3)}(\pi, k)}{kr_{ij}^4} \sin(2kr_{eff} + 2\delta_i(k) - l\pi + \varphi_j^{eff(3)}(\pi, k)) \exp(-2r_{eff}/\lambda(k)) \quad (4b)$$

$$r_{eff} = 2r_{ij}, \text{ (Fig. 2b)}$$

$$\chi_{ijn}^{(3)} = \frac{S_i^2 \mathcal{R} F_{jn}^{eff(3)}(\mathcal{G}_{nij}, k)}{k r_{ij}^2 r_{in}^2} \sin(2k r_{eff} + 2\delta_i(k) - l\pi + \varphi_{jn}^{eff(3)}(\mathcal{G}_{nij}, k)) \exp(-2r_{eff}/\lambda(k)) \quad (4c)$$

$r_{eff} = r_{ij} + r_{in}$  (Fig. 2c)

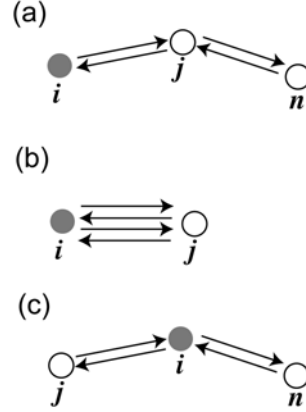


Fig. 2: Schematic representations of triple scattering paths that involve two scatterers (a, c) and a single scatterer (b).

Triple-scattering paths that involve three different scatterers are neglected in the present RMC refinements because of their small effect on the EXAFS signal.

Calculations of the effective amplitude factors and phase corrections are time consuming. Therefore, these characteristics are calculated prior to RMC refinements on the appropriate  $k$  and  $\mathcal{G}$  meshes as described below in Sections 2.2, 2.3. During the refinements, the scattering amplitudes for the intermediate values of  $\mathcal{G}$  are calculated using linear interpolation.

### 2.1.3 Double and Triple Scattering In the Nearly-Collinear Chains

Double- and triple-scattering paths that yield significant contributions to EXAFS involve nearly collinear chains ( $\mathcal{G}_{ijn} < 20^\circ$ ) (Figs. 1, 2) containing the intervening atom (i.e. atom  $j$  in Figs. 1, 2) in the first coordination shell of the absorber. In principle, scattering amplitudes and phase shifts depend on all three angles within the triangle formed by the absorber and the scatterers. However, the present code assumes that for the nearly collinear chains these parameters are determined entirely by the  $\mathcal{G}_{ijn}$  angle; this simplifying, yet sufficiently accurate, assumption was introduced to speed up the calculations. A utility program **EXAFS\_INTER.exe** is used to calculate the amplitudes and phase shifts as a function of  $\mathcal{G}_{ijn}$  on the  $\mathcal{G}$ -mesh selected by the user, and write the resulting data for all the double and triple scattering paths into **\*.n<sub>1</sub>n<sub>2</sub>n<sub>3</sub>c2** and **\*.n<sub>1</sub>n<sub>2</sub>n<sub>3</sub>c3** files, respectively, as detailed in Section 5.2.

### 2.1.4 Double and Triple Scattering In the Nearest Coordination Spheres

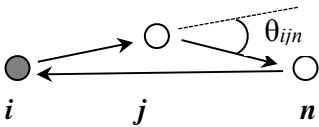
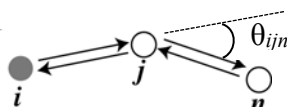
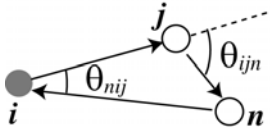
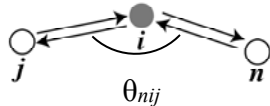
Another important geometry for double scattering involves triangular paths with the scatterers located in the 1<sup>st</sup> and 2<sup>nd</sup> coordinations shells around the absorber (Figs. 1b). In

this case, the effective amplitude factors and phase corrections are determined primarily by the  $\mathcal{G}_{nij}$  angles. Again, a utility program **EXAFS\_INTER.exe** is used to calculate the amplitudes and phase shifts as a function of  $\mathcal{G}_{nij}$  on the  $\mathcal{G}$ -mesh selected by the user (Section 5.3) and store the resulting data for these double-scattering paths in the file **\*.n<sub>1</sub>n<sub>2</sub>n<sub>3</sub>s2**.

The amplitude and phase parameters for the triple-scattering paths shown in Fig. 2b are stored in the file **\*.nsc3**. Similar tables for the triple-scattering paths shown in Fig. 2c are stored in the file **\*.n<sub>1</sub>n<sub>2</sub>n<sub>3</sub>s2**.

## 2.2 The EXAFS files for combined PDF/EXAFS refinements

Below is a list of files required to run RMCProfile with EXAFS data included in the refinements:

Filename	Path pictogram	File Content
<b>*.n<sub>1</sub>sc1</b>		photoelectron mean free path; moduli and phases of backscattering amplitudes for the single-scattering paths;
<b>*.n<sub>1</sub>sc3</b>		amplitude factors and phase corrections for the triple-scattering paths
<b>*.n<sub>1</sub>n<sub>2</sub>n<sub>3</sub>c2</b>		effective amplitude factors and phase corrections for the double-scattering paths in nearly collinear atomic chains
<b>*.n<sub>1</sub>n<sub>2</sub>n<sub>3</sub>c3</b>		effective amplitude factors and phase corrections for the triple-scattering paths in nearly collinear atomic chains
<b>*.n<sub>1</sub>n<sub>2</sub>n<sub>3</sub>s2</b>		effective amplitude factors and phase corrections for the double-scattering paths having both scattering atoms in the 1 <sup>st</sup> and 2 <sup>nd</sup> coordination shells around the absorber
<b>*.n<sub>1</sub>n<sub>2</sub>n<sub>3</sub>s3</b>		effective amplitude factors and phase corrections for the triple-scattering paths with the two scattering atoms located in the 1 <sup>st</sup> coordination shell around the absorber, and the absorber atom itself acting as a scatterer
<b>absorlist.dat</b>		list of absorber atoms around each atom in the configuration
<b>scattlist.dat</b>		list of all scattering atoms for each absorber

In the filenames,  $n_1$  stands for the type of the absorbing atom,  $n_2$  for the type of the distant scatterer, and  $n_3$  for the type of the intervening scatterer in *\*.n<sub>1</sub>n<sub>2</sub>n<sub>3</sub>c2(3)* files; in the files *\*.n<sub>1</sub>n<sub>2</sub>n<sub>3</sub>s2(3)*,  $n_2$  and  $n_3$  represent types of the scattering atoms.

## 2.3 Preparation of EXAFS Data

The following preliminary analyses of EXAFS data are required to obtain accurate values of energy shifts,  $E_0$ , and to subtract the background from the data:

- (a) Use Athena (or similar) to extract EXAFS from the absorption spectra;
- (b) For each experimental EXAFS dataset, build an appropriate cluster(s) around the absorbing atom. An average structure provides a good starting model. Examples of free software that can be used to generate these clusters based on space group and atomic positions include Atoms/Artemis. For structures with the same absorber species located at non-equivalent crystallographic positions, separate clusters must be generated for each site. The non-equivalent sites must be designated using distinct atom types in the \*.rmc6f file. The contributions of these clusters to the total EXAFS signal are set proportional to the respective site occupancies;
- (c) Perform self-consistent FEFF calculations of the scattering paths in a separate folder for each cluster. In the FEFF input file, set the amplitude-reduction parameter  $S_0^2$  to a value less than 0.1 to let FEFF estimate this parameter from the atomic overlap integrals. Identify scattering paths to be used in the fit;
- (d) Use Artemis (or similar) to fit the experimental EXAFS using selected scattering paths. For all the paths, set  $S_0^2$  ('amp' parameter in the Artemis's GDS section) to a value calculated by FEFF and define it as a "set" parameter. FEFF8.20 provides a satisfactory estimate for  $S_0^2$ , which can be found in the header of the **chi.dat** FEFF output file. If this value of  $S_0^2$  results in physically unreasonable values of  $\sigma^2$  and/or poor fit, then  $S_0^2$  can be refined by defining this parameter as "Guess". The fitted value of  $S_0^2$  may deviate from the theoretical value because of various experimental artifacts, such as inhomogeneous samples; significant deviations likely indicate a problem and should be considered seriously. If multiple experimental EXAFS datasets are available, a simultaneous fit is recommended. Each dataset should be assigned a single value of  $E_0$  for all the paths;
- (e) Return to the EXAFS data-reduction software (e.g. Athena) and adjust  $E_0$  to the fitted value to convert EXAFS oscillations from the energy space to  $k$ -space. Repeat the fit in Artemis using these modified data and obtain a new value of  $E_0$ . Repeat this procedure iteratively until  $E_0 < 0.5$  eV. This process minimizes systematic errors caused by the incorrect choice of  $E_0$ ;
- (f) In Artemis, fit the background, if possible, and save the experimental data and the background as chi(k).
- (g) Use any spreadsheet software (e.g. Excel) to subtract the background from the experimental data. The background subtraction option in the current version of Artemis appears to work incorrectly.
- (h) Transform the background-subtracted experimental data into the following format:  
1<sup>st</sup> line – number of experimental points;  
2<sup>nd</sup> line – title;  
Subsequent lines –  $k$  ( $\text{\AA}^{-1}$ ) and chi(k) values in xy format.

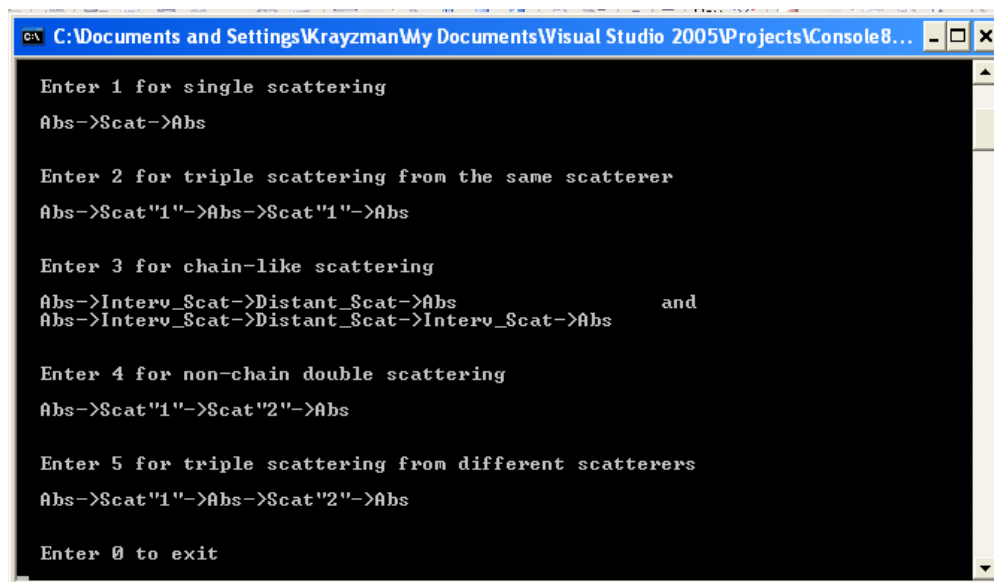
## 2.4 Creating EXAFS files

We use a cubic double perovskite  $\text{SrAl}_{1/2}\text{Nb}_{1/2}\text{O}_3$  to illustrate the procedure. The EXAFS data for Sr and Nb are stored in the files `I_Sr-back.dat` and `I_Nb-back.dat`, respectively. The order of atom types in the `rmc6f` configuration file is 1-Sr, 2-Nb, 3-Al, 4-O. Note that the same chemical species can correspond to different atom types.

Create a separate folder for each absorber type and perform FEFF calculations for all the absorbers.

- Each of these folders should contain the following files/subfolders: (1) `EXAFS_INTER.exe` file, (2) `FEFFxxx.exe` file, (3) experimental EXAFS datafile, (4) **feff.inp** file generated by Artemis, (5) **paths.dat** file generated by FEFF, and (6) a subfolder called “**store**” where the output files will be stored;
- Rename the **paths.dat** file created by FEFF to **pathsbackup.dat**. An example of the **paths.dat** file and the description of its structure are presented in Appendix A1;
- Open **feff.inp** file and change the CONTROL card parameters to  
CONTROL 0 0 0 0 1 1 for FEFF820.exe and FEFF light or to  
CONTROL 0 0 1 1 for FEFF6l.exe
- Identify the paths to be included in the fit;
- Run `EXAFS_INTER.exe`. Respond to the prompts. The “reduction factor” is the  $S_0^2$  parameter obtained in the preliminary fit.

The following menu will appear:



```
C:\Documents and Settings\Krayzman\My Documents\Visual Studio 2005\Projects\Console8...
Enter 1 for single scattering
Abs->Scat->Abs

Enter 2 for triple scattering from the same scatterer
Abs->Scat"1"->Abs->Scat"1"->Abs

Enter 3 for chain-like scattering
Abs->Interv_Scat->Distant_Scat->Abs and
Abs->Interv_Scat->Distant_Scat->Interv_Scat->Abs

Enter 4 for non-chain double scattering
Abs->Scat"1"->Scat"2"->Abs

Enter 5 for triple scattering from different scatterers
Abs->Scat"1"->Abs->Scat"2"->Abs

Enter 0 to exit
```

Select an appropriate option(s) and enter the following information:

### Option 1

Enter a sequence of file numbers xxxx for the feffxxxx.dat files corresponding to representative single-scattering paths for each type of scattering atoms. An output file **\*.n<sub>1</sub>sc1** will be generated.

### Option 2

Enter a sequence of file numbers xxxx for the feffxxxx.dat files corresponding to representative triple-scattering paths, which involve one scattering (not absorbing) atoms and the absorbing atom as the second scatterer. An output file **\*.n<sub>1</sub>sc3** will be generated.

### Option 3

Enter the types of the distant and intervening scatterers for a double-scattering *chain-like* process and the number xxxx of the feffxxxx.dat file corresponding to this forward-scattering path. A value of the scattering angle for the selected path will be displayed. Enter the minimum and maximum values (in degrees) for the angular range to be sampled. An output file **\*.n<sub>1</sub>n<sub>2</sub>n<sub>3</sub>c2** will be generated. Enter the number xxxx of the feffxxxx.dat file corresponding to the triple-scattering path. An output file **\*.n<sub>1</sub>n<sub>2</sub>n<sub>3</sub>c3** will be generated. In order to include similar scattering processes for another set of the distant and intervening scatterers, select option 3 again and follow the same procedure.

### Option 4

Enter the types of scatterers for a non-chain double-scattering process (Fig. 3). Several nonequivalent paths may exist that include the same types of scatterers, which occupy distinct crystallographic positions (see figure below). These paths may exhibit very different internal angles. For example, for an atomic configuration having disordered thermal displacements, the probable ranges of internal angles are 70° – 110° for path *a* and 150° – 180° for path *b*. A single angular range for both paths would yield a mesh that is too coarse for interpolation because each range is divided only into 10 parts.

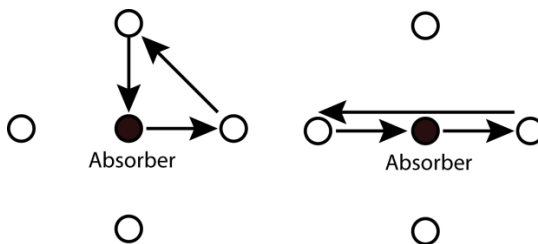


Fig. 3: Examples of non-chain double-scattering paths.

Enter the total number of representative paths and, then, the numbers xxxx of the corresponding feffxxxx.dat files in the ascending order for the internal angle (angle  $\theta_{nij}$  for a triangular path is defined in Fig. 1). As the number of the feffxxxx.dat file corresponding to the smallest angle is entered, a value of this angle will be displayed. Enter the minimum and maximum values (in degrees) for the angular range to be sampled. The procedure should be repeated for every double-scattering path with the specified scatterers. The angular ranges selected for different non-equivalent paths involving the same scatterers should not overlap. In order to specify the double-scattering processes for other types of scatterers select option 4 again.

## Option 5

Enter the types of scatterers for a non-chain triple-scattering process (Fig. 4). Several inequivalent paths may exist that include the same types of scatterers (see comments for option 4). Enter the total number of these paths and, then, the numbers xxxx of the corresponding feffxxxx.dat files in the ascending order of the internal angle (angle  $\theta_{nij}$  for a triangular path is defined in Fig. 1). As the number of a feffxxxx.dat file corresponding to the smallest angle is entered, a value of this angle will be displayed. Enter the minimum and maximum values (in degrees) for the angular range to be sampled. The procedure should be repeated for every distinct triple-scattering path to be included in the fit. The angle intervals selected for different inequivalent paths involving the same scatterers should not overlap. For specifying similar triple-scattering processes for other types of scatterers select option 5 again.

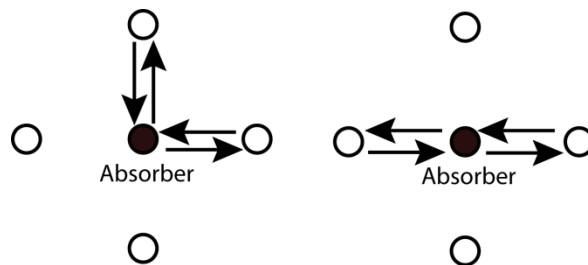


Fig. 4: Examples of non-chain triple-scattering paths

## 2.5 Creating lists of absorbing and scattering atoms

These lists are generated using the utility **SCAT\_ABS.exe** and stored in files **absorlist.dat** (Appendix A2) and **scattlist.dat** (Appendix A3). For running **SCAT\_ABS.exe**, copy the initial configuration file **\*.rmc6f** into a folder which contains **SCAT\_ABS.exe**. In the same folder, create an input file **scat\_input.txt**. An example of the input file is shown below:

```
SrAlNbO3
2 {NATOMICSPECIES} - the total number of different species (i.e., Nb and Sr)
Nb 4.2 0.0 4.2 0.0 4.2 5.0 4.2 0.0
Sr 4.2 0.0 4.0 0.0 4.2 0.0 4.2 0.0
```

The first line provides the name of the rmc6f configuration file in the (omit the extension). The second line specifies the number of experimental EXAFS datasets to be included in the fit plus (if applicable) the number of atomic species to be swapped with the absorbing atoms. That is **NATOMICSPECIES=3** if Nb and Al will be swapped during the fit and **NATOMICSPECIES=2** if no swap moves will be involved. This line is followed by the **NATOMICSPECIES** lines in arbitrary order.

Each of these lines starts with a chemical symbol of the absorbing atom or the atom which will be swapped with the absorber during the fit. This symbol is followed by *n* types pairs of real numbers, where *n* types is the number of types of atoms in the configuration file. The first number in the pair is the maximum distance separating the corresponding

scattering and absorbing atoms to be included in the list. The second number is the maximum scattering angle (in degrees) within which the software will search for an intervening atom for chain-scattering paths that involves these absorber-scatterer pairs. If this number is set to 0.0, the routine will not search for an intervening atom.

NOTE: For the \*.**rmc6f** format, the number of types of atoms is determined automatically from the list of chemical species in the **.dat** file.

### 3. Diffuse scattering in Electron Diffraction

#### 3.1. Diffuse-scattering calculations

The calculations of diffuse scattering were implemented following the formalism proposed by Butler and Welberry (*B. D. Butler, T. R. Welberry, J. Appl. Cryst. 25, 391, 1992*) and later adopted for RMC refinements using electron diffraction by Goodwin *et al.* (*A. L. Goodwin, R. L. Withers, H. B. Nguyen, J. Phys. Cond. Matter, 19(33), 335216, 2007*). According to this formalism, the complex total scattering amplitude  $A_{\text{tot}}(\mathbf{k})$  is calculated in the kinematic approach as

$$A_{\text{tot}}(\mathbf{k}) = \sum_{\mathbf{n}} \sum_{m=1}^M f_m(k) \exp(i\mathbf{k}(\mathbf{R}_{\mathbf{n}} + \mathbf{r}_{m\mathbf{n}})), \quad (6)$$

where  $\mathbf{k}=(k_x, k_y, k_z)$  is the diffraction vector,  $\mathbf{R}_{\mathbf{n}}=(an_x, bn_y, cn_z)$  is a vector that describes the origin of the  $\mathbf{n}^{\text{th}}$  unit cell,  $\mathbf{r}_{m\mathbf{n}}=(x_{m\mathbf{n}}, y_{m\mathbf{n}}, z_{m\mathbf{n}})$  is a vector that describes the position of the  $m^{\text{th}}$  atom in the  $\mathbf{n}^{\text{th}}$  cell,  $f_m(k)$  is the atomic scattering factor,  $a$ ,  $b$ , and  $c$  are the lattice parameters,  $N_x$ ,  $N_y$ , and  $N_z$  specify the number of unit cells along the corresponding axes of the configuration box,  $N=N_xN_yN_z$  is the total number of the unit cells in the box, and  $M$  is the number of atoms in the unit cell,  $0 \leq n_\alpha \leq N_\alpha - 1$  ( $\alpha \in [x, y, z]$ )

The average scattering amplitude  $\langle A(\mathbf{k}) \rangle$  is calculated as

$$\langle A(\mathbf{k}) \rangle = \frac{1}{N} \sum_{\mathbf{n}} \sum_{m=1}^M f_m(k) \exp(i\mathbf{k}(\mathbf{r}_{m\mathbf{n}})). \quad (7)$$

The amplitude of diffuse scattering  $A_D(\mathbf{k})$  is a difference

$$A_D(\mathbf{k}) = A_{\text{tot}}(\mathbf{k}) - \langle A(\mathbf{k}) \rangle \psi(\mathbf{k}), \quad (8)$$

where the interference function  $\psi(\mathbf{k})$  is

$$\psi(\mathbf{k}) = \sum_{\mathbf{n}} \exp(i\mathbf{k}\mathbf{R}_{\mathbf{n}}) = \frac{\exp(ik_x a N_x) - 1}{\exp(ik_x a) - 1} \cdot \frac{\exp(ik_y b N_y) - 1}{\exp(ik_y b) - 1} \cdot \frac{\exp(ik_z c N_z) - 1}{\exp(ik_z c) - 1}. \quad (9)$$

The intensity of diffuse scattering is  $I_D(\mathbf{k}) = \ln|A_D(\mathbf{k})|^2$ . The intensities in experimental electron diffraction patterns are affected by multiple scattering and therefore cannot be reproduced by calculations that rely on the kinematic approximation. Therefore, only the

locus of diffuse scattering, which reflects the topology of correlations in real space, is fitted; the information on the magnitude of correlation parameters can be recovered only to the extent that is encoded in the total scattering and EXAFS data. In the present fitting procedure, the experimental (relative units) and calculated intensities are matched using the scale factor and the offset which are adjusted after each RMC move.

Typically, the total scattering amplitude calculated for a single atomic configuration by direct summation (6) is too noisy to be used in the fit. In the present software, the noise is reduced using the following procedure which relies on the periodic boundary conditions imposed in the RMC refinements. The position of an atom in the configuration is described by a sum  $\mathbf{R}_n + \mathbf{r}_{mn}$ . Therefore, the transformation of the atomic coordinates according to the formulae

$$\begin{aligned}
 an_x + x_{mn} &\rightarrow \begin{cases} a(n_x - l_x) + x_{mn} & \text{for } l_x \leq n_x < N_x \\ a(n_x - l_x + N_x) + x_{mn} & \text{for } 0 \leq n_x < l_x \end{cases} \\
 bn_y + y_{mn} &\rightarrow \begin{cases} b(n_y - l_y) + y_{mn} & \text{for } l_y \leq n_y < N_y \\ b(n_y - l_y + N_y) + y_{mn} & \text{for } 0 \leq n_y < l_y \end{cases}, \\
 cn_z + z_{mn} &\rightarrow \begin{cases} c(n_z - l_z) + z_{mn} & \text{for } l_z \leq n_z < N_z \\ c(n_z - l_z + N_z) + z_{mn} & \text{for } 0 \leq n_z < l_z \end{cases}
 \end{aligned} \tag{10}$$

generates the atomic configuration that is equivalent to the original. The total scattering amplitude calculated for the new configuration using Equation (6) is somewhat different compared to that calculated for the original configuration, whereas the average scattering amplitude remains unchanged. According the present procedure, the  $I_D(\mathbf{k})$  calculated after each RMC move is averaged over eight equivalent configurations with  $l_x=0, [N_x/2]$ ;  $l_y=0, [N_y/2]$ ;  $l_z=0, [N_z/2]$ . The maximum number of equivalent configurations that could be included in the averaging is  $N$ , but using so many configurations would make the computations prohibitively expensive.

### 3.2 Atomic scattering factor calculations

The atomic scattering factors for electron diffraction are calculated using the traditional parameterization per the formula (Peng L-M, Acta Cryst., A54, 481, 1998)

$$f_m(k) = \sum_{j=1}^5 a_j \exp(-b_j k^2) + \frac{me^2}{8\pi^2 \hbar^2 k^2} \Delta Z, \tag{11}$$

where  $a_j$  and  $b_j$  are the tabulated parameters (Peng L-M, Acta Cryst., A54, 481, 1998),  $\Delta Z$  represents the ionic charge, the pre-factor  $\frac{me^2}{8\pi^2 \hbar^2} = 0.023934$  if  $k$  is given in  $\text{\AA}^{-1}$  and  $f_m(k)$  is in  $\text{\AA}$ . The values of  $a_j$  and  $b_j$  are stored in the file **FormfactorsTable.dat**. The **FormfactorsTable.dat** consists of three-line blocks for each type of atoms in the configuration. The first line in a block is a chemical symbol for a given atom type, the second line contains five real values of  $a_j$ , and the third line contains five real values of  $b_j$ .

The order of blocks in the file is not important. The file may include the blocks for atoms not participating in a given configuration. A user can modify this file in any text editor. Ionic charges (valences) should be specified as real numbers in the **\*.dat** file after the keyword “VALENCE ::”. The valences must be listed in the same order as the atoms in the “ATOMS ::” line.

**NO\_BACKGROUND ::**

### 3.3 Input and output files

The input files **diffilename.ext**, (**.ext** is an arbitrary 3-character extension), each containing a distribution of diffuse intensity, for a set of given sections of reciprocal space to be included in the fit, are produced using the **ED.exe** utility program from the digitized experimental electron diffraction patterns. The procedure for generating these input files is detailed in Section 3.4. The first line of the input file contains an integer **nline** which specifies the number of data lines in the file followed by an integer **nsec**, which specifies the number of equivalent sections of reciprocal space used for averaging of the calculated signal. Each of the following lines contains two integer numbers, specifying pixel coordinates of a given point, and the **nsec** groups of three real numbers describing its reciprocal-space coordinates (in  $\text{\AA}^{-1}$ ) and the corresponding intensity value.

Four kinds of the output files are produced for each diffraction pattern used in the fit. The graphic files **diffilename\_exper.bmp** and **diffilename\_calc.bmp** facilitate visual comparison of the experimental and calculated patterns for each dataset. A digital output is provided in the files **diffilename\_exper.dat** and **diffilename\_calc.dat**. The “**exper**” files contain experimental diffuse scattering patterns for control purposes. “**Calc**” files, which contain diffuse scattering patterns calculated for the current atomic configuration, are saved along with the output files for other data. The first three lines in **diffilename\_calc.dat** files contain the residual, the scale factor, and the offset for a given dataset. (A consecutive number of the dataset is shown in parentheses.) These lines are followed by a matrix describing the intensity distribution.

If an optional subordinate card “SAVE ::” is present in any of the ‘DIFFUSE\_SCATTERING ::’ keyword blocks, the output files **diffilename\_calc.bmp** and **diffilename\_calc.dat** are saved under the names **diffilename\_calc-n.bmp** and **diffilename\_calc-n.dat**, where **n** is a consecutive ascending two-digit number; otherwise, the old output files are replaced with the new ones.

### 3.4. Processing of input files

If experimental diffraction patterns containing diffuse scattering are recorded on a film, they must be digitized using a suitable scanner or a similar device and stored in the **.bmp** format. The processing of the resulting image to produce an input data file for RMCProfile involves the following steps:

- a) Define the origin of a coordinate system for the image and determine it’s coordinates;

- b) Define two reciprocal space vectors in the image;
- c) Mask all the Bragg peaks which will be excluded from the fit;
- d) Choose an appropriate quarter of the diffraction pattern to be used in the fit.

The central spot in experimental electron diffraction patterns is saturated and, as such, is not suitable for precise determination of the origin. Instead, the center is found from the coordinates of several Bragg peaks located symmetrically around the central spot. The program **ED.exe** prompts the user to select suitable Bragg spots using mouse clicks. The program fits each of these peaks with a 2-D Gaussian (saturated portions of the peaks, if encountered, are excluded by the program) to find the peak positions. The position of the origin is calculated as an average of the Bragg peak positions.

The two reciprocal space vectors are defined (following the on-screen prompts) by using mouse clicks to select several orders for the two independent reflection families (e.g. 111, 222, 333 and 100, 200, 300) and specifying the *hkl* indexes for each of these peaks. The program automatically determines the precise positions of the selected peaks and the length of the corresponding reciprocal space vectors in  $\text{\AA}^{-1}$ .

The RMCProfile code fits only the diffuse component of electron scattering and, therefore, Bragg peaks must be excluded from the fitted pattern. This is accomplished by using masks which are placed on top of all the Bragg spots in the pattern. The mask has an ellipsoidal shape inscribed into a rectangular. The user selects the size of the mask by defining the upper left and lower right corners of this rectangular using mouse clicks as prompted by the program. Once the user selects one Bragg peak, the program automatically locates and masks its pair related by the 180° rotation around the centre.

Finally, the user selects a quarter of the diffraction pattern to be included in the fit (only one quarter is fitted to reduce the computational time) using a mouse click in the corresponding corner of the diffraction pattern. Once this action is complete, the program ED.exe creates the input file for RMCProfile. The name of this file must be specified under the “DIFFUSE\_SCATTERING ::” card of the **\*.dat** file.

#### 4. Restraints on peak tails and line curvature in partial PDFs

“DISTANCE WINDOW” and “MINIMUM DISTANCES” constraints frequently cause unphysical spikes/discontinuities in partial PDFs. The effects are most pronounced for two closely overlapped partial PDFs having opposite signs of their respective Faber-Ziman coefficients. The artificial spikes in such PDFs cancel each other so that the total PDF exhibits no discontinuities; therefore, no driving force for “healing” of these spikes exists. The problem can be mitigated by imposing restraints on relevant peak tails in the partial PDFs using the following sigmoidal function:

$$B(r) = \frac{A_1 - A_2}{1 - \exp\left(\frac{r - r_0}{\Delta r}\right)} + A_2 \quad (5)$$

where  $A_1$  and  $A_2$  should be set to zero for the low- $r$  and high- $r$  tails of the peak, respectively. Other coefficients are determined by fitting  $B(r)$  to the tail(s) of the peak of interest in the partial  $g_m(r)$ . This can be accomplished using any suitable graphing software (e.g., Origin).

For each tail restraint, a user specifies the  $r_{\min}$  (left) and  $r_{\max}$  (right) limits of the interval over which the constraint is applied plus parameters  $A_1$ ,  $A_2$ ,  $r_0$ , and  $\Delta r$  of the sigmoidal function  $B(r)$ .

The restraint for a low- $r$  tail is activated by including the following block of keywords in the \*.dat file:

```
LEFT_TAILS ::  
> START_FINISH :: here,  $r_{\min}$  and  $r_{\max}$  for this tail must be specified  
> PARTIAL :: an integer corresponding to the number of a partial  
> COEFFICIENTS :: 4 real numbers describing coefficients  $A_1$ ,  $A_2$ ,  $r_0$ , and  $\Delta r$   
> WEIGHT :: a weight assigned to the penalty function
```

The restraint for a high- $r$  tail is activated using similar keywords with the major keyword RIGHT\_TAILS ::.

Once the restraint is activated, after each atomic move, RMCProfile checks the inequality  $g_m(r_i) > B(r_i)$  for all  $r_j \in [r_{\min}, r_{\max}]$  and, if the condition is satisfied, the penalty function having a user-specified weight is added to the residual.

Another way to suppress unphysical features in the partials is to constrain their curvature.

This restraint is activated using the card

```
CURVATURE ::  $n$   $r_1$   $r_2$   $w$ 
```

which imposes a penalty proportional to the integral of the absolute value of the second derivative of the  $n^{\text{th}}$  partial over the interval  $[r_1, r_2]$ . The weight  $w$  determines the contribution of this restraint to the total residual.

## **5. Off-centering of B-cations, macroscopic polarization, and distributions of [BO<sub>6</sub>] octahedral volumes in perovskite structures**

### **5.1 Off-centering of transition-metal cations in octahedral coordination**

For studies of an atomic structure in ferroelectric crystals it is important to determine the displacements of positively charged metal cations relative to the negatively charged oxygens. For  $3d$  transition metals in octahedral coordination, the displacement of a metal cation from the instantaneous center of an octahedron is reflected in the pre-edge structure of the metal  $K$ -edge X-ray absorption spectra (XAS). The intensity  $I_B(\alpha)$  of the relevant pre-edge peak is proportional to the average square of the metal off-centering as:

$$I_B(\alpha) \propto \left\langle \left( r_\alpha^M - \frac{r_\alpha^{O_1} + r_\alpha^{O_2}}{2} \right)^2 \right\rangle / d_\alpha^{5.5}, \quad (6)$$

where  $\alpha$  is the coordinate along the octahedron's diagonal along which the polarization vector of a linearly polarized X-ray beam is oriented,  $r_\alpha^j$  are the coordinates of the  $j^{\text{th}}$  atom,  $d_\alpha$  are the average octahedron dimensions,  $O_1$  and  $O_2$  are the nearest-neighbor oxygen atoms around the transition-metal cation along the  $\alpha$  axis. As follows from the formula (6) the average off-centering

$$\xi_\alpha = \sqrt{\left\langle \left( r_\alpha^M - \frac{r_\alpha^{O_1} + r_\alpha^{O_2}}{2} \right)^2 \right\rangle} \quad (7)$$

is determined by the three-body distribution function.

In polycrystalline samples, the intensity of the pre-edge peak is

$$I_B(\text{ceramics}) = 1/3(I_B(x) + I_B(y) + I_B(z)) \quad (8)$$

The present implementation permits the fit of the off-centering for a single type of octahedral metal cations in either cubic or tetragonal structures; for the latter, a tetragonal axis must be aligned with the  $z$  axis of the atomic configuration. The fit is activated using the following card in the **.dat** file:

**PRE\_EDGE** ::  $n_1$   $n_2$   $\xi$   $w_1$   $\zeta$   $w_2$

where the integers  $n_1$  and  $n_2$  are the consecutive numbers of types of the absorbing metal atom and the ligands, and real  $\xi$  is the desired value of the 3d off-centering in Å

$$\xi = \sqrt{\left\langle \left( r_x^M - \frac{r_x^{O_1} + r_x^{O_2}}{2} \right)^2 \right\rangle + \left\langle \left( r_y^M - \frac{r_y^{O_3} + r_y^{O_4}}{2} \right)^2 \right\rangle + \left\langle \left( r_z^M - \frac{r_z^{O_5} + r_z^{O_6}}{2} \right)^2 \right\rangle}, \quad (9)$$

$w_1$  is the weight of the contribution of this data into the residual,  $\zeta$  is the desired maximum of the off-centering variance in Å<sup>2</sup>,  $w_2$  is the corresponding weight.

If single crystal data are available, with the measurements performed by aligning the polarization vector of an X-ray beam with both a and c tetragonal axes, one can specify the ratio of the corresponding pre-edge peak intensities,  $A$ . This is accomplished using the following card:

**ANISOTROPY** ::  $a$

which enables separate fitting of the off-centering in the directions parallel and perpendicular to the tetragonal axis.

Since  $\xi_x^2 + \xi_y^2 + \xi_z^2 = \xi^2$ ,  $\xi_x = \xi_y$ , and  $\xi_z^2 / \xi_x^2 = a$

$$\xi_x = \xi_y = \sqrt{\frac{\xi^2}{2+a}}, \quad \xi_z = \sqrt{a}\xi_x$$

The off-centering is recalculated after each move of either the metal or oxygen atoms.

The penalty (determined by  $w_2$ ) is added to the residual if the variance of the off-centering in any direction  $\langle \xi_\alpha^2 \rangle - \langle \xi_\alpha \rangle^2$  exceeds  $\zeta$ .

## 5.2 Input and output files for off-centering

Fitting of the metal-cation off-centering is currently applicable to perovskite structures with either cubic or tetragonal symmetry. The lists of oxygen atoms surrounding each transition metal and of transition-metal atoms around each oxygen are stored in the file **stemname.pre** that must be present in the working directory. If a PRE\_EDGE :: card is present in the \*.dat file, the file **stemname.pre** will be created automatically from the \*.rmc6f file.

The first part of the **stemname.pre** file is a six-column table in which each line contains the numbers of six oxygen atoms forming an octahedron around the given metal atom in the order of X+, X-, Y+, Y-, Z+, Z- (where *e.g.* X+ is an oxygen atom displaced relative to the metal atom along the x axis in the positive direction. The second part of the file is a two-column table in which each line contains the number of the absorbing metal atoms which reside within the octahedra having the corresponding oxygen atom as a common vertex. If the octahedron contains a metal atom of another (non-absorbing) type, the number of that atom is set to “zero”.

The output file **Pre-edge\_distr.dat** is a four-column table in which each line below the header contains three values of  $r_\alpha^M - \frac{r_\alpha^{O1} + r_\alpha^{O2}}{2}$  for  $\alpha=x, y,$  and  $z$ , followed by the metal off-centering value  $\zeta$  for the corresponding absorber. If the ANISOTROPY card is present, the header contains target values for  $\zeta_x, \zeta_y,$  and  $\zeta_z$ , their calculated values, and the corresponding variances; otherwise, only the calculated and target values of the off-centering are specified. The output file is calculated for the starting atomic configuration prior to the fit and then updated/saved after a user-specified run time along with the other output files.

## 5.3 Macroscopic polarization

A macroscopic polarization for a ferroelectric crystal with a perovskite  $ABO_3$  structure or solid solutions  $(A_xA'_{1-x})BO_3$  is calculated and fitted if the following card is present in the .dat file:

POLARIZATION ::  $\psi$  w Q(B)  $Q_{\text{long}}(\text{oxygen})$   $Q_{\text{trans}}(\text{oxygen})$  Q(A) [Q(A')]

where  $\psi$  is the experimental value of polarization in  $C/m^2$ , w is the weight factor, Q(B) is the Born charge of the B-cations,  $Q_{\text{long}}(\text{oxygen})$  and  $Q_{\text{trans}}(\text{oxygen})$  are the “longitudinal” and “transverse” Born charges of oxygen, and Q(A) is the Born charge of the A-cations. The order of atoms in the .rmc6f file should be: 1-B-cations, 2-oxygen, 3- A cations and,

if solid solutions, 4-A-cations. If there are 4 types of atoms in the \*.rmc6f file, the Born charge of the second A-cations should be specified as well.

## 5.4 Distributions of octahedral volumes

The off-centering of B-cations correlates with the volume of the oxygen octahedron. The user can fit the average octahedron volume and the variance of the volume distribution to the desired values using the card

OCTAHEDRON :: V w<sub>1</sub> VAR w<sub>2</sub>

where V is the target octahedron volume in Å<sup>3</sup>, VAR is the variance of the volume distribution in Å<sup>6</sup>, w<sub>1</sub> and w<sub>2</sub> are the corresponding weight parameters. This option requires the card PRE\_EDGE :: since the code uses the **stemname.pre** file.

## 6. Miscellaneous

The card CRYSTALMAKE\_OUT :: generates the output file in the format readable by Crystal Maker. The entire configuration is folded onto a single unit cell.

The subordinate keyword > WEIGHTED RESIDUAL in the group BRAGG :: changes the form of the residual used for the Bragg profile to the weighted. In this case the residual R is calculated according to the formula

$$R = \sum_i \frac{(I_{\text{exp}}(t_i) - I_{\text{calc}}(t_i))^2}{\sqrt{I_{\text{exp}}(t_i)}^2}$$

## 7. Major keywords in the \*.dat file

EXAFS ::	Introduces a block of keywords for an EXAFS dataset. Text can follow the :: but will be ignored. This keyword must be followed by a block of subordinate keywords. Each EXAFS spectrum requires a separate keyword and a block of data. <i>Do not include if no EXAFS data are fitted.</i>
LEFT_TAILS :: / RIGHT_TAILS ::	Introduces a block of keywords for peak tail restraints in partial PDFs. This keyword must be followed by a block of subordinate keywords. <i>Do not include if no restraints are used.</i>
DIFFUSE_SCATTERING ::	Introduces a block of keywords for fitting electron diffuse scattering. Text can follow the :: but will be ignored. This keyword must be followed by a block of subordinate keywords. Each diffraction pattern requires a separate keyword and a block of data. <i>Do not include if no electron diffraction data are fitted.</i>

VALENCE ::  $V_1 \dots V_{n_{types}}$   
 LINEAR ::  
 LOGARITHMIC ::  
 BOX\_SIZE ::  $N_x N_y N_z$   
 NO\_BACKGROUND ::  
  
 PRE-EDGE ::  
 OCTAHEDRON ::  
 POLARIZATION ::  $\psi w Q_B Q_l Q_t Q_A$   
 [Q<sub>A</sub>]  
  
 CRYSTALMAKE\_OUT ::  
 CURVATURE ::

## 8. Subordinate keywords in the \*.dat file

EXAFS ::

> FILENAME ::	Filename containing the data
>FIT_SPACE ::	Acceptable values: $r$ , $k$ ( <i>case-insensitive</i> ). Specifies whether a real (coordinate) space or a wave-vector space ( $k$ ) is used for the EXAFS fit.
> START_POINT_(R_SPACE) ::	Start point for a fit in the $r$ space (Å)
> END_POINT_(R_SPACE) ::	End point for a fit in the $r$ space (Å)
> R_SPACING ::	Value of the spacing used in the EXAFS fit and the output (Å).
> LOW_R_REGION_LIMIT::	(Optional) If specified, assigns additional factor to the lower- $r$ part contribution to the total misfit. This factor must be provided with the subordinate keyword >LOW_R_WEIGHT
> LOW_R_WEIGHT ::	An additional factor for the lower- $r$ part contribution to the total misfit in the case of $r$ -space fit
> START_POINT_(K_SPACE) ::	Start point of the fit in $k$ -space (if selected in >FIT_SPACE) or a Fourier transform for a fit in the $r$ space (Å <sup>-1</sup> )
> END_POINT_(K_SPACE) ::	End point of the fit in $k$ space or a Fourier transform for a fit in the $r$ space (Å <sup>-1</sup> )
> K_POWER ::	Specifies the power of $n$ in the weight-factor $k^n$ used to multiply EXAFS signal $\chi(k)$ prior to a Fourier transform
> WEIGHT ::	Parameter to weight the total misfit for the EXAFS data in Monte Carlo simulation

> ENERGY_OFFSET ::	(Optional) Shift of $E_0$ (eV) in the experimental spectrum. If not included, $E_0=0$
> SCALE_FACTOR ::	(Optional) Scale factor for the experimental spectrum (optional). If not included, scale factor=1
> NUMBER_OF_TYPES_OF_ABSORBING_ATOMS::	(Optional) Specifies the number of types of absorbing atoms for a given EXAFS dataset. If not included, the number of types is set to 1.
> TYPE(S)_OF_ABSORBING_ATOMS::	A list of types of the absorbing atoms for a given EXAFS dataset

LEFT\_TAILS :: (RIGHT\_TAILS ::)

> START_FINISH ::	$r_{min}$ and $r_{min}$ values (Å)
> PARTIAL ::	Number of partials to which the restraint is applied
> COEFFICIENTS ::	Coefficients $A_1$ , $A_2$ , $r_0$ , and $\Delta r$ in Equation (5)
> WEIGHT ::	Weight of the penalty function due to the tail restraint

DIFFUSE\_SCATTERING ::

> FILENAME ::	Filename containing the data
> WEIGHT ::	Parameter to weight the total misfit for the diffuse scattering data in Monte Carlo simulation.
> SAVE ::	(Optional)

BRAGG ::

> WEIGHTED_RESIDUAL ::	
------------------------	--

## Appendix

### A1. The Pathsbackup.dat file

```
...
Rmax 6.0000, keep limit 0.000, heap limit 0.000 Feff 6L.02 paths 3.05
Plane wave chi amplitude filter 2.50%
```

```
-----
  1  2  6.000  index, nleg, degeneracy, r= 1.9805
    x      y      z  ipot  label  rleg  beta  eta
0.000000  0.000000  1.980540  4  'O  '  1.9805  180.0000  0.0000
0.000000  0.000000  0.000000  0  'Nb '  1.9805  180.0000  0.0000

  2  2  8.000  index, nleg, degeneracy, r= 3.3764
    x      y      z  ipot  label  rleg  beta  eta
-1.949350  1.949350 -1.949350  1  'Sr  '  3.3764  180.0000  0.0000
0.000000  0.000000  0.000000  0  'Nb '  3.3764  180.0000  0.0000

  3  3  24.000  index, nleg, degeneracy, r= 3.3810
    x      y      z  ipot  label  rleg  beta  eta
1.980540  0.000000  0.000000  4  'O  '  1.9805  135.0000  0.0000
0.000000 -1.980540  0.000000  4  'O  '  2.8009  135.0000  0.0000
0.000000  0.000000  0.000000  0  'Nb '  1.9805   90.0000  0.0000

  4  2  6.000  index, nleg, degeneracy, r= 3.8987
    x      y      z  ipot  label  rleg  beta  eta
0.000000 -3.898700  0.000000  3  'Al  '  3.8987  180.0000  0.0000
0.000000  0.000000  0.000000  0  'Nb '  3.8987  180.0000  0.0000

  5  3  12.000  index, nleg, degeneracy, r= 3.8987
    x      y      z  ipot  label  rleg  beta  eta
0.000000  0.000000 -3.898700  3  'Al  '  3.8987  180.0000  0.0000
0.000000  0.000000 -1.980540  4  'O  '  1.9182   0.0000  0.0000
0.000000  0.000000  0.000000  0  'Nb '  1.9805  180.0000  0.0000

  6  4  6.000  index, nleg, degeneracy, r= 3.8987
    x      y      z  ipot  label  rleg  beta  eta
-1.980540  0.000000  0.000000  4  'O  '  1.9805   0.0000  0.0000
-3.898700  0.000000  0.000000  3  'Al  '  1.9182  180.0000  0.0000
-1.980540  0.000000  0.000000  4  'O  '  1.9182   0.0000  0.0000
0.000000  0.000000  0.000000  0  'Nb '  1.9805  180.0000  0.0000
```

### A2. The absorlist.dat file

```
20480  total number of lines equal to the total number of atoms in cfg
14      maximal number of absorbers in a line
10 4097 2  4609 2  5121 2  5633 2  2049 1  2056 1  2561 1  2617 1  3073 1
3521 1
10 4098 2  4610 2  5122 2  5634 2  2049 1  2050 1  2562 1  2618 1  3074 1
3522 1

8  194 1  706 1  1218 1  1730 1  2242 1  2754 1  3266 1  3778 1

14 4609 2  5057 2  ...      ...  576 1  1480 1  2041 1  2056 1  2617 1  3521 1
4096 1
```

### A3: The scattlist.dat file

```
6144 total number of lines equals the number of atoms in the configuration.
26 maximal number of scatterers in a line
26 2049 1 0 0 ... 3073 1 0 0

20 181 1 0 0 .....6901 3 10933 4 7349 3 13493 ..... 20149 4 0 0
```

### A4. Example of a combined fit of neutron total PDF, Bragg profile, and electron diffuse scattering

The cubic phase of perovskite-like  $\text{KNbO}_3$  is believed to exhibit 8-site displacive disorder associated with random local displacements of Nb along 8 non-equivalent  $\langle 111 \rangle$  directions. The displacements are correlated along the -Nb-O-Nb- linear chains parallel to  $\langle 100 \rangle$  directions. Similar 8-site disorder is encountered in perovskite  $\text{BaTiO}_3$  and  $\text{AgNbO}_3$  as well as their solid solutions with other perovskite compounds. The correlated displacements are manifested in three orthogonal sets of  $\{100\}$  sheets of diffuse intensity passing through all the fundamental reflections; the diffuse intensity is extinct through the origin of reciprocal space because the correlated displacement components are directed parallel to the correlation directions. In the present example we used synthetic data simulated for a large atomic configuration that mimicked the 8-site disorder for Nb to determine whether the correct displacement correlations can be recovered at least using error-free data. The simulated data that was used in these analyses included neutron PDF and electron diffuse scattering.

The structure model used to simulate the data was based on the configuration cell of  $64 \text{ \AA} \times 64 \text{ \AA} \times 64 \text{ \AA}$ , which contained 20,480 atoms located at the ideal lattice sites of the cubic perovskite structure. The Nb atoms were shifted along  $\langle 111 \rangle$  directions  $0.1\sqrt{3} \text{ \AA}$  and the O atoms were shifted along  $\langle 001 \rangle$  direction by  $0.1 \text{ \AA}$  to generate positive Nb-Nb and negative Nb-O displacement correlations along the  $\langle 001 \rangle$  -Nb-O-Nb-  $\langle 001 \rangle$  chains; the displacements among different chains remained uncorrelated thus yielding the desired 8-site model (Figure A4.1). Subsequently, all atoms in the configuration were subjected to random Gaussian displacements. The total neutron pair-distribution function (PDF) and Bragg profile were calculated for this model configuration and used instead of experimental datasets in the RMC fits.

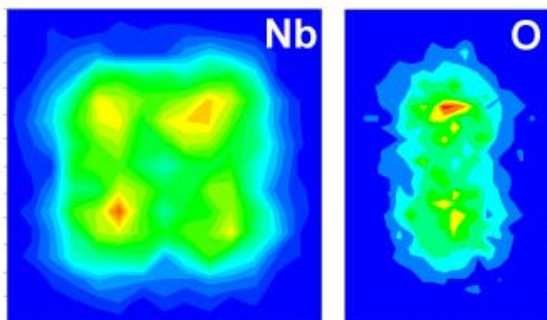


Figure A4.1: Probability density distribution functions for Nb and O viewed down  $\langle 100 \rangle$  directions in the 8-site  $\text{KNbO}_3$  model. A splitting of the atomic positions due to correlated atomic displacements is observed.

First, a combined fit of the neutron PDF and Bragg profile was performed starting from the ideal lattice sites. The fit produced discernable negative correlations among the nearest-neighbor Nb and O displacements which were evident in the doublet structure of the first peak in the total PDF. Despite an excellent agreement between the target and calculated data, the magnitude of the Nb-O correlations was much smaller compared to the target value. More importantly, the refined configuration exhibited no Nb-Nb and O-O correlations but instead featured positive K-K correlations, which were absent in the target model. No noticeable correlations existed beyond 4 Å. Clearly, the local structure obtained using powder total scattering data alone is grossly incorrect even though the 8-site and 2-site splitting was reproduced to some extent for the Nb and O probability density distribution functions, respectively. The fit also produced reasonable agreement between the calculated and target variances  $\langle u^2 \rangle$  for all the atomic positions. Unquestionably, without a prior knowledge of the structural, an incorrect model would have been inferred from RMC refinements using the neutron total scattering data.

In the second attempt, the neutron PDF and Bragg profile were complemented by the two electron diffraction patterns containing diffuse scattering. The results of a simultaneous fit of these four datasets are presented in Figure A4.2.

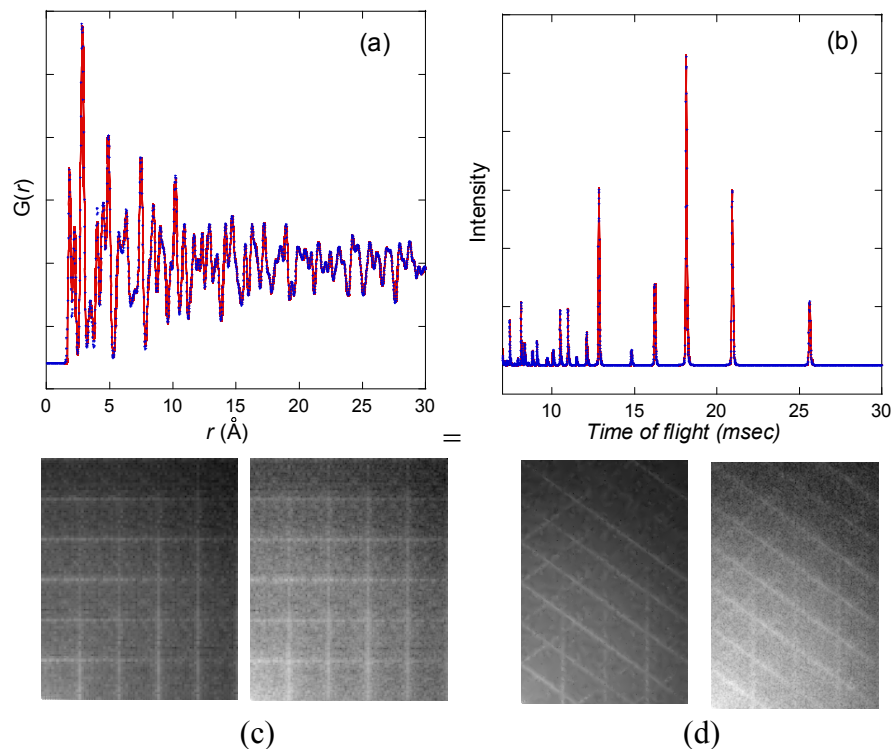


Figure A4.2: Results of a simultaneous fit of the neutron PDF and Bragg profile and electron diffuse scattering (two sections). (a, b) Experimental (blue) and calculated (red) neutron PDF (a) and Bragg profile (b). Experimental (left) and calculated (right) electron diffuse scattering patterns in the (130) (c) and (114) (d) sections of reciprocal space.

Now, the displacement correlations were reproduced in the refined configuration, although the correlation strengths were still significantly weaker than the target values. In particular, positive Nb-Nb and O-O displacement correlations were recovered and the

incorrect K-K correlations, while still present, decreased considerably. Clearly, including the information encoded in electron diffraction improved considerably a correctness of the recovered displacement correlations.